Pure & Appl.Chem., Vol.55, No.3, pp.479-492, 1983.
Printed in Great Britain.

0033-4545/83/030479-14$03.00/0
Pergamon Press Ltd.

FLUID MIXTURES AT HIGH PRESSURES

Gerhard M. Schneider

Department of Chemistry, University of Bochum, Bochum,
Federal Republic of Germany

Abstract - In the present survey some important trends in the high pressure thermodynamics of fluid mixtures of non-electrolytes are reviewed.

First the pressure dependence of excess functions such as the excess Gibbs energy G^E, the excess enthalpy H^E, the excess entropy S^E, and the excess heat capacity C_p^E is discussed. They can be obtained from a knowledge of the excess volume V^E as a function of pressure, temperature, and composition. Experimental results demonstrate that the variations of V^E as a function of pressure can be important and that even a change of the sign of V^E with increasing pressure has been found in some cases. The pressure dependence of H^E values thus obtained agree well with literature values determined from direct flow-calorimetric measurements.

Until now most thermodynamic information has had to be deduced from high-pressure phase equilibria and critical phenomena where our knowledge is much better. The pressure dependence and critical phenomena of liquid-gas, liquid-liquid, and gas-gas equilibria will be shortly reviewed. Mainly binary systems will be treated, but phase-separation phenomena in some ternary systems will also be considered.

New developments during recent years have shown that the limits between liquid-gas, liquid-liquid, and gas-gas equilibria are not well defined and that continuous transitions occur. This continuity will be demonstrated on recent results for binary mixtures of hydrocarbons with tetrafluoromethane and nitrogen.

Methods for the calculation and correlation of high-pressure phase equilibria in fluid mixtures under pressure are reviewed. They start from equations of state or from theories of mixtures using sometimes rather complicated mixing rules for the mixture parameters. Some results are presented and compared with experimental data.

The significance of high-pressure phase equilibria in fluid mixtures for practical applications is briefly discussed e.g. for fluid extraction, supercritical fluid chromatography (SFC), and for some high-pressure techniques and processes.

INTRODUCTION

Section 6 of this Conference is concerned with the thermodynamics of fluid mixtures at high pressures. Whereas many research activities have already been dedicated to the high-pressure properties of pure compounds, the high-pressure thermodynamics of mixtures is still in a developing state.

In the present review some important trends in the high-pressure thermodynamics of fluid mixtures of non-electrolytes will be discussed. It is the aim to show that at high pressures interesting and sometimes new effects are found that often allow a better understanding of the enormous amount of knowledge that has already been obtained at normal pressure. The present written version of the lecture will have an accent on recent results mostly obtained in the author's laboratory at the University of Bochum during the last two or three years and will accordingly be a continuation of some older of our review ar-

ticles in this field (15-23). Additionally the author will try to give a synopsis of the 14 poster contributions to Section 6 of this Conference (1-14).

EXCESS FUNCTIONS AT HIGH PRESSURE

Whereas the temperature dependence of excess functions of liquid mixtures has been widely investigated, knowledge about the pressure dependence of excess functions is still poor.

The p-dependence of the molar excess Gibbs energy $\underline{G}_m^E$, the molar excess entropy $\underline{S}_m^E$, and the molar excess enthalpy $\underline{H}_m^E$ can be obtained from accurate measurements of the molar excess volume $\underline{V}_m^E$ as a function of temperature and pressure, according to the well-known thermodynamic relations:

$$(\partial \underline{G}_m^E/\partial \underline{p})_{\underline{T},\underline{x}} = \underline{V}_m^E \tag{1}$$

$$(\partial \underline{S}_m^E/\partial \underline{p})_{\underline{T},\underline{x}} = -(\partial \underline{V}_m^E/\partial \underline{T})_{\underline{p},\underline{x}} \tag{2}$$

$$(\partial \underline{H}_m^E/\partial \underline{p})_{\underline{T},\underline{x}} = \underline{V}_m^E - \underline{T}\cdot(\partial \underline{V}_m^E/\partial \underline{T})_{\underline{p},\underline{x}} \tag{3}$$

Here $\underline{V}_m^E$ is defined as

$$\underline{V}_m^E(\underline{T},\underline{p},\underline{x}) \equiv \underline{V}_m(\underline{T},\underline{p},\underline{x}) - \{\underline{x}_1\cdot\underline{V}_{m1}^*(\underline{T},\underline{p}) + \underline{x}_2\cdot\underline{V}_{m2}^*(\underline{T},\underline{p})\} \tag{4}$$

where $\underline{V}_m(\underline{T},\underline{p},\underline{x})$ is the molar volume of a mixture of mole fraction $\underline{x}$ at given temperature and pressure and $\underline{V}_{m1}^*(\underline{T},\underline{p})$ and $\underline{V}_{m2}^*(\underline{T},\underline{p})$ are the molar volumes of pure components 1 and 2 at given temperature and pressure respectively.

Integration of equations (1) to (3) yields the change of the molar excess functions between atmospheric pressure and the pressure $\underline{p}$ for a mixture at given temperature and mole fraction:

$$\underline{G}_m^E(\underline{p}) - \underline{G}_m^E(0.1\ \text{MPa}) = \int_{0.1\ \text{MPa}}^{\underline{p}} \underline{V}_m^E\, d\underline{p} \tag{5}$$

$$\underline{S}_m^E(\underline{p}) - \underline{S}_m^E(0.1\ \text{MPa}) = -\int_{0.1\ \text{MPa}}^{\underline{p}} (\partial \underline{V}_m^E/\partial \underline{T})_{\underline{p},\underline{x}}\, d\underline{p} \tag{6}$$

$$\underline{H}_m^E(\underline{p}) - \underline{H}_m^E(0.1\ \text{MPa}) = \int_{0.1\ \text{MPa}}^{\underline{p}} \{\underline{V}_m^E - \underline{T}\cdot(\partial \underline{V}_m^E/\partial \underline{T})_{\underline{p},\underline{x}}\} d\underline{p} \tag{7a}$$

$$= \underline{G}_m^E(\underline{p}) - \underline{G}_m^E(0.1\ \text{MPa}) - \underline{T}\{\underline{S}_m^E(\underline{p}) - \underline{S}_m^E(0.1\ \text{MPa})\} \tag{7b}$$

To evaluate equations (5) to (7) it is necessary to measure $\underline{V}_m^E$ as accurately as possible. $\underline{V}_m^E$ can be obtained in two ways:

(1) indirectly by measuring densities of pure liquids and their mixtures at known compositions, or

(2) directly by observing the change in volume when two pure liquids are mixed in a dilatometer.

From measurements at atmospheric pressure it is well-known that direct measurements of $\underline{V}_m^E$ are capable of yielding higher-precision results more readily than the indirect method. In our measurements we therefore adopted method (2) whereas the first was used by Dymond et al. in their poster presentation (5).

Our excess-volume measurements were performed in a stainless-steel dilatometer of the batch type, mounted in a high-pressure autoclave. The apparatus has been improved several times and is described in its present form in detail elsewhere (25). Accuracies for $\underline{V}_m^E$ of about $\pm 0.01\ \text{cm}^3\ \text{mol}^{-1}$ are obtained.

With this apparatus $\underline{V}_m^E$ measurements up to a maximum pressure of about 250 MPa were performed on aqueous solutions of 3-methylpyridine (24), acetonitrile (25,29), acetone (25,29), dioxane (25,29), methanol (25,29), ethanol (25,29), 2-propanol (25,29), glycol (25,29), and pyridine (25,29), as well as on toluene + methylcyclohexane (27), 2-propanol + heptane (27), tetradecafluorohexane

+ hexane (28), ethanol + methylcyclopentane (31), hexane + octane (30), + decane (30), + dodecane (30), + tetradecane (30), octane + tetradecane (30), and decane + tetradecane (30).

In Fig.1 and 2 some recent results on three very different types of binary mixtures are presented:

- alkane + alkane e.g. hexane + octane, + decane, + dodecane (see Fig.1a and 1b) (32)
- alcohol + alkane e.g. 2-propanol + heptane, 2-methoxy-ethanol + heptane (see Fig.2a) (32)
- alcohol + water e.g. 2-propanol + H_2O, 2-butanol + H_2O (see Fig.2b) (32)

For a review of less recent results see references 19 and 21.

In Fig.1 and Fig.2 $V_m^E(p)$ isotherms for a given mole fraction are presented. The common feature is that the absolute value of V_m^E approaches zero with increasing pressure. Only for 2-butanol + H_2O a slight change of the sign of V_m^E from negative to positive is found, a hint for the possible existence of high-pressure immiscibility phenomena (24). Changes of the sign of V_m^E have also been observed in aqueous solutions of 3-methylpyridine (24), acetonitrile (25, 29), and pyridine (25,29).

The $V_m^E(p)$ isotherms can be correlated with equations that resemble some rather simple ones for V_m of pure compounds, e.g. Tait-like and Hayward-like equations have been used (25,27,29,30-32). The $V_m^E(p)$ isotherms of the n-alkane binaries in Fig.1a and 1b could also be represented rather well by a (somewhat modified) Prigogine-Flory-Patterson treatment (PFP); the results of the theory are given as full lines in Fig.1a and 1b (32).

For an equation of state for liquid mixtures it should therefore be better not to correlate $V_m(p)$ isotherms of a mixture of given composition according to the (mostly very complicated) equations developed for pure substances such as is normally done in the literature but to correlate V_m^E separately according to a normally much simpler equation for V_m^E and only to add the contributions of the pure substances according to Eq (4).

From the V_m^E values the excess Gibbs energy G_m^E can be calculated as a function of pressure according to Eq (5) (25,27,29,30,31). Some very recent results are plotted in Fig.3. For the alkane mixtures where G_m^E is negative at normal pressure G_m^E becomes even more negative for increasing pressures, and for the alcohol + alkane mixtures where G_m^E is positive at normal pressure G_m^E even increases with rising pressure; thus with increasing pressure these mixtures become less ideal with respect to G_m^E (Fig.3) but more ideal with respect to V_m^E (Fig.1 and 2). The G_m^E values for 2-propanol + H_2O and 2-butanol + H_2O being positive at normal pressure, however, decrease with increasing pressure (Fig.3). Thus these systems become more ideal with increasing pressure with respect to G_m^E (Fig. 3) as well as to V_m^E (Fig.2b); as a consequence the mutual miscibility increases with rising pressure.

From Eq (6) and Eq (7) S_m^E and H_m^E can be determined as a function of pressure from V_m^E measurements; some results are given in references 25 and 29. As a recent example H_m^E data for 2-propanol + heptane that were obtained from V_m^E measurements according to Eq (7) are plotted against pressure in Fig.4 and are compared with H_m^E values that were determined directly from high-pressure flow calorimetry by Heintz (33). The agreement is within the limits of experimental error.

Direct calorimetric H_m^E measurements in a flow calorimeter at high pressures are a very promising development of high-pressure experimental techniques. This is demonstrated by the two poster presentations by Christensen et al. (6) and Oswald et al. (7) at this Conference. Further progress in this field is greatly to be encouraged.

HIGH-PRESSURE PHASE EQUILIBRIA OF FLUID MIXTURES

Normally the three different types of two-phase equilibrium in fluid mixtures namely liquid-liquid, liquid-gas, and gas-gas equilibria are discussed separately. During the last decade, systematic investigations, however, have shown that the limits between these three forms of heterogeneous phase equilibrium are not well defined and that continuous transitions occur. This hypothesis has been discussed in detail in several reviews (15-23) where also references are given. Thus only a short treatment will be presented here.

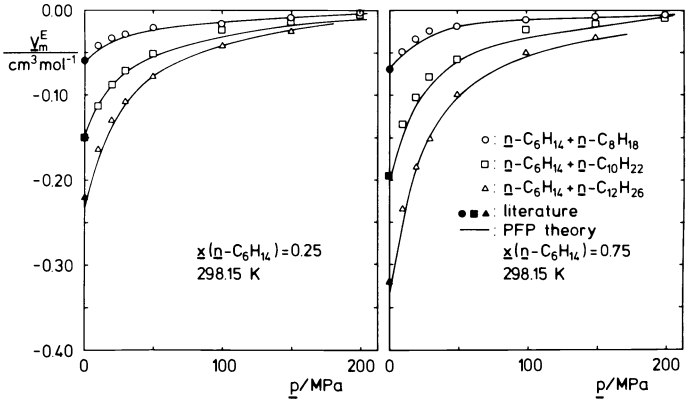

Fig. 1a Fig. 1b

Fig. 1. Molar excess volumes V_m^E as a function of pressure p in binary n-alkane mixtures at 298.15 K. From measurements by Hess (32) (see text).

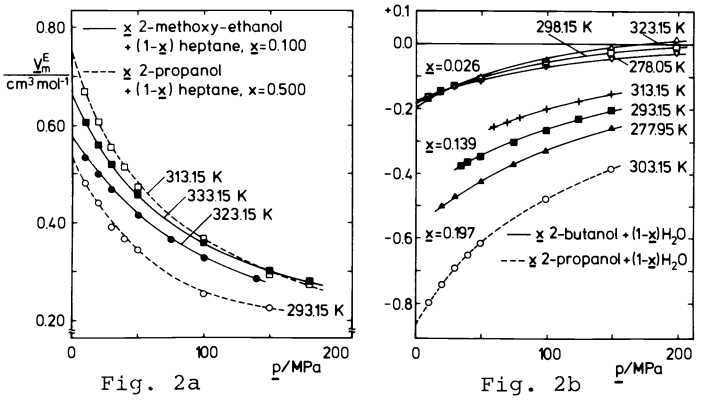

Fig. 2a Fig. 2b

Fig. 2. Molar excess volumes V_m^E as a function of pressure p at different temperatures. From measurements by Hess (32).

Fig. 2a. Binary alcohol + alkane mixtures.

Fig. 2b. Binary alcohol + water mixtures

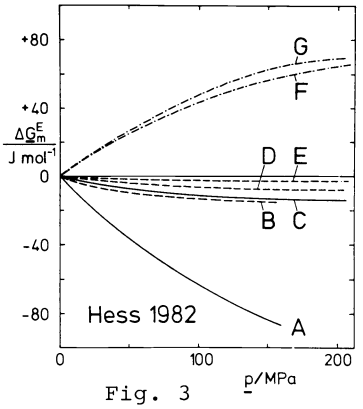

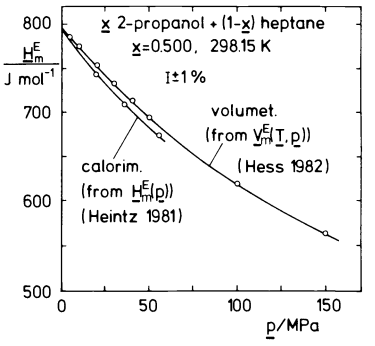

Fig. 3 Fig. 4

Fig. 3. Change of the molar excess Gibbs energy G_m^E as a function of pressure ($\Delta G_m^E \equiv G_m^E(p) - G_m^E(0.1\ \text{MPa})$). A, x2-propanol + (1-x)H_2O, x = 0.197, 303.15 K. B, xdodecane + (1-x)hexane, x = 0.250, 298.15 K. C, x2-butanol + (1-x)H_2O, x = 0.025, 298.15 K. D, xdecane + (1-x)hexane, x = 0.250, 298.15 K. E, xoctane + (1-x)hexane, x = 0.250, 298.15 K. F, x2-propanol + (1-x)heptane, x = 0.500, 303.15 K. G, x2-methoxy-ethanol + (1-x)heptane, x = 0.100, 333.15 K. From measurements by Hess (32).

Fig. 4. Molar excess enthalpy H_m^E as a function of pressure for 2-propanol + heptane. Upper curve: from V_m^E measurements (32). Lower curve: from high-pressure flow calorimetry (33) (see text).

The discussion starts from Fig.5 where the phase behaviour and the critical phenomena are schematically represented for a binary mixture exhibiting separation into two liquid phases. For the type in Fig.5a and 5b the critical curve liquid-gas (lg) is not interrupted and runs through the usual pressure maximum. At temperatures far below the critical temperature of the pure volatile component I separation into two liquid phases additionally takes place. The branch ll of the critical curve corresponds to upper critical solution temperatures (UCST) as a function of pressure that are slightly raised with increasing pressure in the case shown.

An example for this type is found in the system Kr + CHF_3 for which some isobaric $\underline{T}(\underline{x})$ sections are given in Fig.6. Here the UCSTs increase with increasing pressure. At about 230 MPa, the liquid-liquid miscibility gap will disappear below the crystallization surface. An additional interesting feature of this system is that two liquid phases coexist with solid CHF_3 at low pressures (e.g. at 0.1 MPa) but with solid Kr at higher pressures (e.g. at 100 and 200 MPa) resulting in a quadruple point between 0.1 MPa and 100 MPa where two liquid phases, solid Kr and solid CHF_3 are in equilibrium; this unusual phase behaviour is caused by the intersection of the melting-pressure curves of pure Kr and pure CHF_3.

Liquid-liquid equilibria have been studied under pressure rather frequently. Important thermodynamic information can be deduced from such investigations, e.g. about the signs of $(\partial^2 \underline{Z}^E_m/\partial \underline{x}^2)_{\underline{T},\underline{p}}$ or even of $\underline{Z}^E$ itself where $\underline{Z}^E = \underline{H}^E, \underline{S}^E$, or $\underline{V}^E$. The effects have already been reviewed several times (15-19,21). The pressure dependence of closed immiscibility loops in the isobaric $\underline{T}(\underline{x})$ diagram is especially interesting; they can e.g. disappear or even appear with increasing pressure. These effects have also been used for the investigation of the kinetics of phase separation in liquid mixtures by pressure jump experiments (37-39). For spectroscopic investigations in liquid mixtures e.g. on H-bonding see reference 36.

Crystallization diagrams have also been investigated as a function of pressure. Some recent results are shown in Fig.7 where isobaric $\underline{T}(\underline{x})$ diagrams are given for CF_4 + xenon, CF_4 + krypton, and CF_4 + argon (35,46). As demonstrated by the nearly horizontal slope of the $\underline{T}(\underline{x})$ isobars of the CF_4 + xenon system in the middle composition range it can be deduced that this system is not far from a liquid-liquid phase separation, this tendency, however, decreasing with increasing pressure. From such measurements the pressure dependence of the excess Gibbs energy and of activity coefficients can also be calculated (35,46).

The more the mutual miscibility of the two components decreases the more the branch ll of the critical curve in Fig.5a and 5b will be displaced to higher temperatures. It can finally penetrate the ranges of temperature and pressure for the critical phenomena liquid-gas (lg) and may pass continuously into the critical line lg whereas the branch of the critical curve starting from the critical point CPI of pure component I ends at a critical endpoint C on the three-phase line liquid-liquid-gas (llg) (Fig.5c and 5d). For still lower mutual miscibility of the components critical-locus curves may be obtained such as those indicated in Fig.5d by dotted lines (e.g. without any pressure maximum and minimum or running directly to increasing temperatures and pressures). Since these types are attributed to gas-gas equilibria, continuous transitions between liquid-gas, liquid-liquid, and gas-gas equilibria should be possible.

In order to prove this hypothesis, series of binary systems were studied where one constant component I such as carbon dioxide (21,40,42), methane (21), ethane (40), ethylene (40), water (21,41), etc. was combined with a component II that was systematically altered in size, shape, structure, and/or polarity, the phrase "family" being proposed for such a series of related binary systems.

As an example the $\underline{p}(\underline{T})$ projections of the phase diagrams of some members of the carbon dioxide family are presented in Fig.8 (42). Here the fluid phase behaviour of the system CO_2 + octane corresponds to the type of Fig.5a and 5b whereas CO_2 + hexadecane and CO_2 + squalane (or 2,6,10,15,19,23-hexamethyltetracosane) have to be attributed to systems belonging to the type given in Fig.5c and 5d (full line). CO_2 + tridecane corresponds to a transition type. Phase behaviour and critical phenomena in CO_2 systems have been extensively discussed in the literature (16,17,19-23,40,42, etc).

In Fig.9 some data for the CF_4 family are compiled. Here our recent results on CF_4 + propane (11,46,47), CF_4 + butane (11,46,47), CF_4 + heptane (11,50),

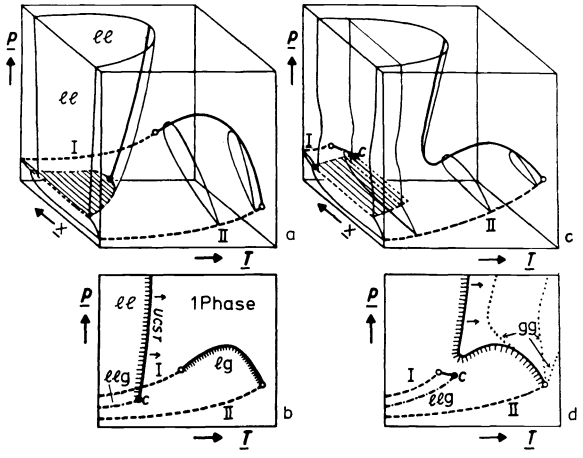

Fig. 5.

Phase equilibria in fluid binary mixtures (schematic) (see text).
Fig. 5a and 5c: p,T,x phase diagram
Fig. 5b and 5d: p(T) projection

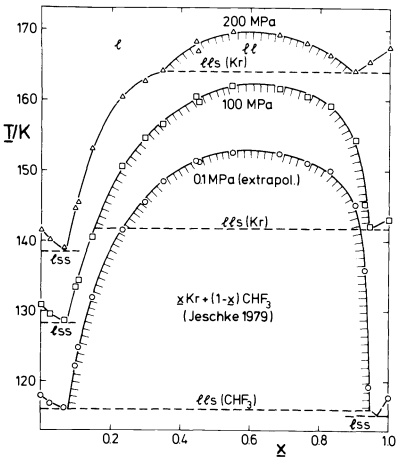

Fig. 6.

Pressure dependence of liquid-liquid phase equilibria: T(x) isobars for x krypton + (1-x) trifluoromethane. From measurements by Jeschke (34).

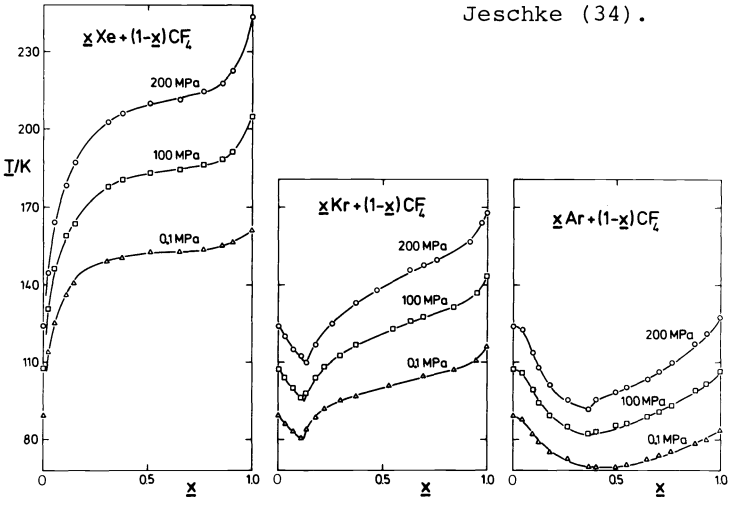

Fig. 7. Pressure dependence of crystallization diagrams of rare gas + tetrafluoromethane mixtures. From measurements by Jeschke (35).

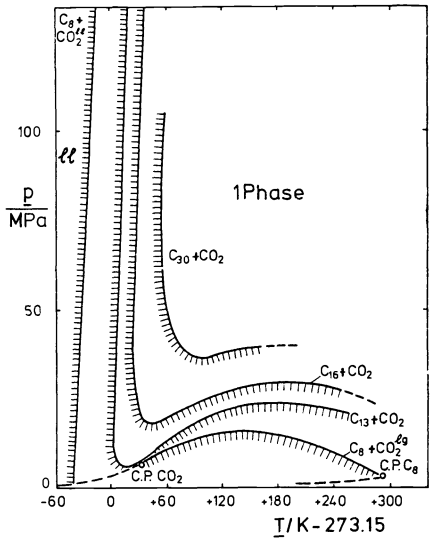

Fig. 8.

Critical locus curves of binary carbon dioxide + alkane mixtures (see text) (42) (C_8 = octane, C_{13} = tridecane, C_{16} = hexadecane, C_{30} = squalane (2,6,10,15,19,23-hexamethyltetracosane)).

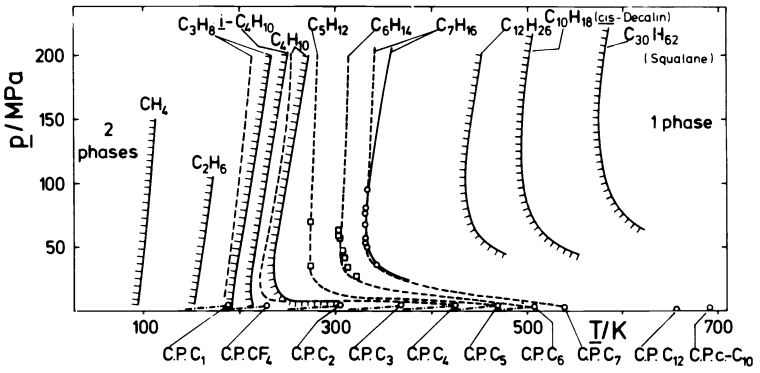

Fig. 9.

Critical locus curves of binary tetrafluoromethane + n-alkane mixtures. Full lines = experimental (44-50), dashed lines = calculated from corresponding-states treatment (49) (see text). For comparison the critical locus curves of CF_4 + 2-methylpropane(isobutane)(55), + cis-decalin (50), and + squalane(2,6,10,15,19,23-hexamethyltetracosane) (50) are also given.

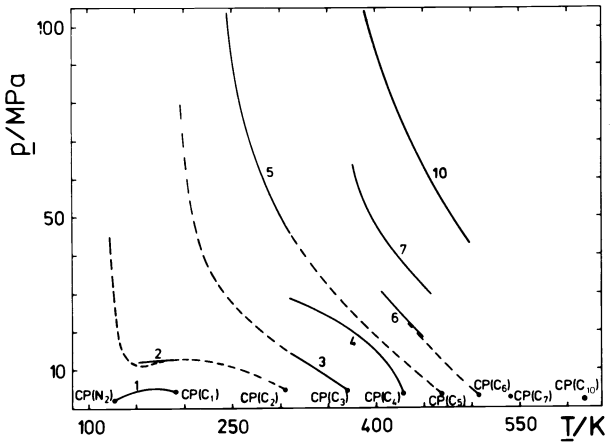

Fig. 10.

Critical locus curves of binary nitrogen + n-alkane mixtures.
Full lines = experimental (50-57), dashed lines = calculated from Redlich-Kwong equation (87) (see text).

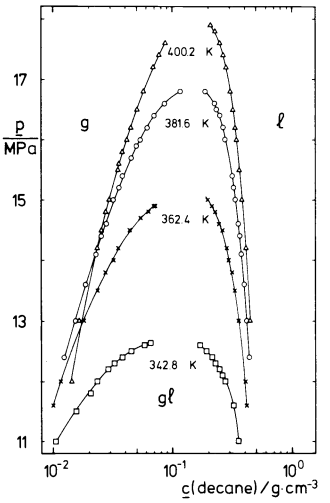

Fig. 11.

p(c) isotherms of decane + carbon dioxide (c = mass concentration of decane in the coexisting phases, logarithmic scale). From measurements by Swaid (58,59).

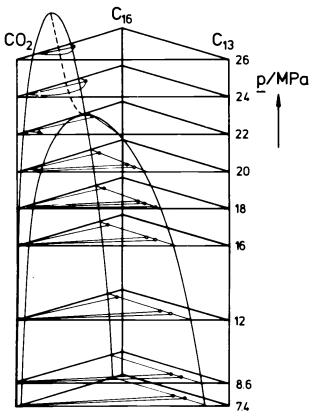

Fig. 12a

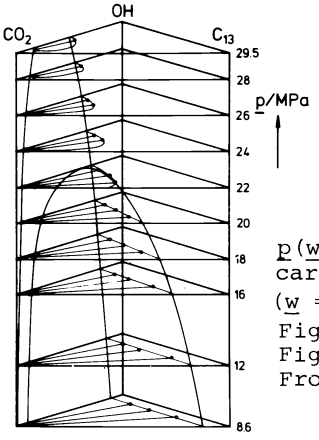

Fig. 12b

Fig. 12.

p(w) phase diagrams of ternary carbon dioxide mixtures at 423.4 K. (w = mass fraction; see text).
Fig. 12a. CO_2 + tridecane + hexadecane
Fig. 12b. CO_2 + tridecane + 1-hexadecanol
From measurements by Konrad (59,60).

CF_4 + dodecane (11,5O), CF_4 + cis-decalin (11,5O), and CF_4 + squalane (11,5O) are compared with our less recent results or data taken from the literature for CF_4 + methane (44), CF_4 + ethane (45), CF_4 + pentane (48), CF_4 + hexane (48), and CF_4 + heptane (49). According to Fig.9 CF_4 + methane, + ethane, and + propane belong to the type given in Fig.5a and 5b the critical curve ll being well separated from the critical curve lg whereas for all other systems the critical curves ll and lg overlap resulting in a whole pattern of critical curves according to Fig.5c and 5d. It is of interest that from such a phase-theoretical discussion the whole variety of phase behaviour and critical phenomena can be understood ranging from a liquid system showing quite normal liquid-liquid immiscibility (e.g. CF_4 + methane, + ethane) up to typical gas solubility systems (e.g. CF_4 + dodecane, + squalane).

The phase relationships in the N_2 family shown in Fig.1O are very similar. Whereas the critical curve lg of $N_2 + CH_4$ (51) is not interrupted, the system N_2 + ethane (52), N_2 + propane (53), N_2 + butane (54), N_2 + pentane (11,55), N_2 + hexane (56), N_2 + heptane (57), and N_2 + decane (11,5O) exhibit critical curves that resemble the types in Fig.5c and 5d without showing, however, any temperature minimum in the range of the experiments. The results for N_2 + pentane (11,55) and N_2 + decane (11,5O) have only recently been obtained in this laboratory. According to the poster presentation by Heintz et al. (1O) the critical phase behaviour of H_2 + ethylene and H_2 + ethane is very similar to that of the N_2 binaries shown in Fig.1O; here, however, the critical curves end at critical endpoints on the three-phase line liquid-liquid-solid respectively within the experimental range.

In Fig.11 some $p(c)$ isotherms for CO_2 + decane (58,59) are given where c is the decane mass concentration; the abscissa is on a logarithmic scale. Here the concentrations of the coexisting phases have been determined directly in a spectroscopic high-pressure cell mounted in a CARY 17H spectrometer in the NIR range using Beer's law. Thus Fig.11 demonstrates that the mutual solubility rapidly increases with increasing pressure and is even complete above the critical pressures of about 12.5 MPa at 342.8 K or 18 MPa at 4OO.2 K. The intersection of isotherms such as shown in Fig.11 is an expected effect in mixtures of this kind, no intersections being found in density(mass concentration) plots at constant temperature.

In Fig.12 isothermal $p(w)$ diagrams are given for the ternary system CO_2 + tridecane + hexadecane (Fig.12a) and CO_2 + tridecane + 1-hexadecanol (Fig.12b) (59,6O) at a constant temperature of 423.4 K where w is the mass fraction. They were measured according to the analytical method by sampling and GC analysis. The curves in the front and the left back side of the prisms represent the borderlines of the two-phase regions of the binary systems (e.g. in Fig. 12a CO_2 + tridecane and CO_2 + hexadecane respectively). The dotted line in Fig. 12a is the critical curve of the isothermal ternary system. For both ternary systems the mutual miscibility of the organic compounds and carbon dioxide increases rapidly with increasing pressure and even becomes complete at conditions above the critical curve whereas the separation factor α defined by $\alpha \equiv (w^g_{C13}/w^l_{C13})/(w^g_{C16}/w^l_{C16})$ only changes slightly, α being about unity near the critical curve and increasing somewhat with decreasing pressures. Therefore pure CO_2 is often a good solvent but less useful for separations.

CALCULATION OF HIGH-PRESSURE PHASE EQUILIBRIA IN FLUID MIXTURES

The continuity between all types of two-phase equilibria in fluid mixtures demonstrated in the preceding section is also of interest from a theoretical point of view especially for the calculation of high-pressure phase equilibria in fluid mixtures.

These calculation methods start from the fact that the conditions for phase equilibrium and for critical points are essentially the same for all types of two-phase equilibria in fluid mixtures. For a binary system the conditions for phase equilibrium are given in Eq(8a) or Eq(8b)

$$G_m' - x_i'(\partial G_m/\partial x_i)'_{p,T} = G_m'' - x_i''(\partial G_m/\partial x_i)''_{p,T} \qquad (8a)$$

or

$$\mu_i' = \mu_i'' \qquad (8b)$$

with

$i = 1$ or 2 for $T' = T''$ and $p' = p''$

and for a binary critical point in Eq(9).

$$(\partial^2 \underline{G}_m/\partial \underline{x}_i^2)_c = 0 \qquad (\partial^3 \underline{G}_m/\partial \underline{x}_i^3)_c = 0 \qquad (9)$$

for i = 1 or 2

From the phase equilibrium conditions the phase diagram is deduced, while from the conditions of a critical point the critical curve can be obtained. In most cases, however, the simple conditions for the molar Gibbs energy $\underline{G}_m$ given in Eq(8)and Eq(9)are not applicable but the more complicated corresponding conditions for the molar Helmholtz energy $\underline{A}_m$ have to be used. Because of difficulties in the definition of standard states generally no excess functions can be applied.

For the calculation and correlation of fluid phase equilibria and critical curves the following methods have been used:

Empirical methods. Here correlations have been developed that are (normally) not based on thermodynamics, e.g. for hydrocarbon mixtures that are of interest for the petroleum and gas industry (61,62).

Methods based on equations of state. Here for the pure components and the mixtures $\underline{A}_m$ or the chemical potentials $\underline{\mu}_i$ are determined from an equation of state e.g. van der Waals, Redlich-Kwong (66), BWR, etc. using (sometimes rather complicated) combination rules (67) for the parameters of the mixtures. In Fig.13 results for Ne + Kr obtained by Trappeniers et al. (63) are compared with data that have been calculated from a new equation of state (64,65). Thus Fig.13 demonstrates that even gas-gas equilibria can be calculated from an equation of state with good accuracy. For details see (19,21,23,61,64).

Theoretical treatment. Theoretical approaches (e.g. lattice models, corresponding-states treatments, perturbation methods, etc.) are of increasing importance. A detailed discussion is outside the scope of this article; for details see e.g. references 49 and 68.

In Section 6 of this Conference the poster presentations by Deiters (12) and Keller et al. (14) are concerned with these problems.

EXPERIMENTAL

Experiments on fluid mixtures at high pressures have become possible only because of the rapid development of experimental techniques during the last decades. In all references given above that concern experimental work informations about techniques, apparatus, etc. can be found; for reviews with respect to the determination of fluid phase equilibria see references 69 and 70, such set-ups being also presented in some posters of Section 6 of this Conference (8-11). The results plotted in Fig.11 and 12 have been obtained with two different set-ups working according to the analytical method where in the first samples are taken and analyzed (e.g. by GC) (59,60) whereas in the second concentrations are determined spectroscopically in NIR using Beer's law (58, 59). For an interesting optoelectronic method see (71).

APPLICATIONS

Fluid mixtures, especially in the critical and supercritical region, are becoming increasingly important in many fields.

Fluid aqueous mixtures at high pressures are of fundamental interest in geology and mineralogy, e.g. in the formation and migration of minerals, gases, or petroleum in the mantle of the earth, for research on volcanos and geysers, for hydrothermal synthesis, etc.

In astronomy and space research, fluid phase equilibria of mixtures (e.g. also gas-gas equilibria) may play an important role in the atmosphere of some planets.

In chemistry highly compressed supercritical gases are of increasing importance as reaction media of continuously variable density, dielectric constant, and solvent power; here the supercritical gas can be solvent as well as reactant, e.g. ethylene, ammonia, carbon dioxide, and even chlorine or fluorine. They are also of interest for some industrial high-pressure syntheses, e.g. of ammonia, methanol, acetic acid, polyethylene, as well as in the oxo synthesis, the Fischer-Tropsch process, and others.

Fluid-phase equilibria at high pressures are of fundamental importance in the

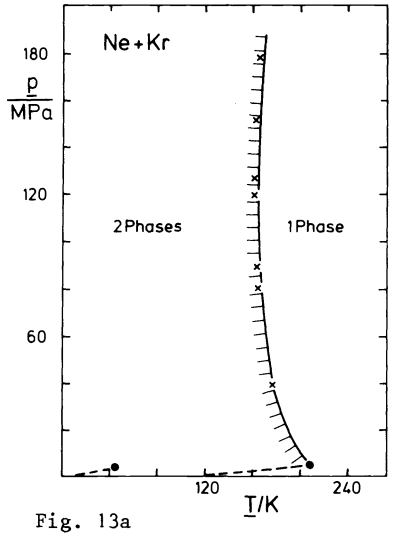

Fig. 13a

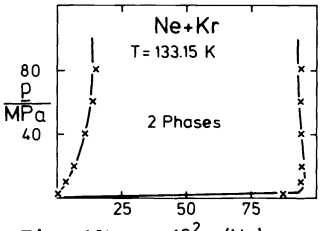

Fig. 13b $10^2 \underline{w}$(Ne)

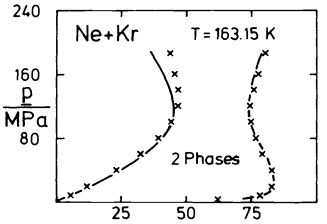

Fig. 13c $10^2 \underline{w}$(Ne)

Fig. 13. Critical locus curve (Fig. 13a) and $\underline{p}(\underline{w})$ isotherms (Fig. 13b and 13c) of Ne + Kr. x = experimental (63), full lines = calculated (64,65) (see text). From calculations by Deiters (64,65).

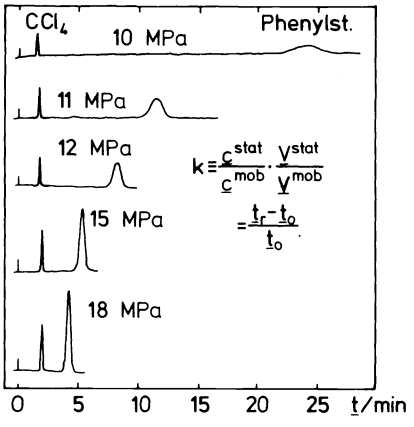

Fig. 14

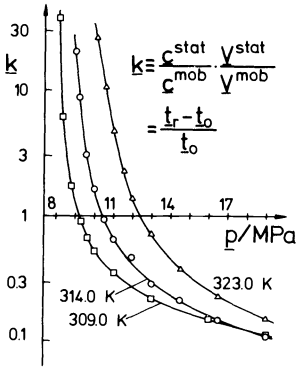

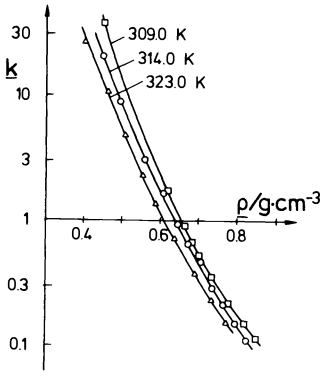

Fig. 15

Fig. 14. Chromatograms of a solution of phenyl stearate and CCl_4 in heptane at 313.8 K and at various pressures.
Mobile phase: CO_2, $\dot{\underline{V}}$(NTP) = 0.4 $dm^3.min^{-1}$
Stationary phase: Perisorb A, column dimensions 25.8 cm x 0.45 cm.
From measurements by Wilsch (77 - 79).

Fig. 15. Capacity ratios $\underline{k}$ of phenyl stearate as a function of pressure $\underline{p}$ (Fig. 15a) and density $\underline{\rho}$ (Fig. 15b) of the mobile phase at various temperatures.
Mobile phase: CO_2, $\dot{\underline{V}}$(NTP) = 0.4 $dm^3.min^{-1}$
Stationary phase: Perisorb RP8, column dimensions 25.6 cm x 0.45 cm.
From measurements by Wilsch (77 - 79).

petroleum and natural as well as synthetic natural gas industry, e.g. for the exploitation of wells, for tertiary oil recovery, for separation and purification methods (also under cryogenic conditions), or for the storage and transport of products.

Important applications are some new separation methods. Decaffeination of coffee and extraction of hops with supercritical carbon dioxide are already used on an industrial scale. Supercritical solvents for the extraction of nicotine, spices, drugs, perfumes, fruit juices, etc. have already been applied. Even extractions of soya beans, ethanol, coal, lubricants, etc. are considered. For an extensive discussion of these problems see references 22, 23 and 72 to 75 where references are also given.

In supercritical fluid chromatography (SFC) compressed gases in the region of their critical temperatures are used as mobile phases. This method was developed in the early sixties and is advantageous for separating low-volatile and thermolabile substances. SFC is also of interest for fundamental research in fluid extraction because it can be used to determine some physico-chemical properties of fluid systems e.g. capacity ratios, diffusion coefficients, etc. For a review and references see reference 76.

As an example, for capacity-ratio measurements chromatograms of a solution of phenyl stearate and CCl_4 in heptane at various pressures are shown in Fig.14 at a constant temperature of 313.8 K that is about 9 K above the critical temperature of pure carbon dioxide (77-79). Here the retention time decreases drastically with increasing pressure.

From these experiments capacity ratios $\underline{k}$ were calculated according to

$$\underline{k} \equiv \frac{\underline{c}^{stat}}{\underline{c}^{mob}} \cdot \frac{\underline{V}^{stat}}{\underline{V}^{mob}} = \frac{\underline{t}_R - \underline{t}_o}{\underline{t}_o} \qquad (10)$$

where $\underline{c}^{stat}$ and $\underline{c}^{mob}$ are the concentrations of the sample and $\underline{V}^{stat}$ and $\underline{V}^{mob}$ the volumes of the stationary and mobile phases respectively and $\underline{t}_R$ and $\underline{t}_o$ the retention time of the substance under test (here phenyl stearate) and the dead time of a non-retained compound (here CCl_4) respectively. According to Eq (10) the capacity ratio $\underline{k}$ is proportional to the distribution coefficient $K \equiv \underline{c}^{stat}/\underline{c}^{mob}$, and since $\underline{V}^{stat}/\underline{V}^{mob}$ is about constant, $\underline{k}$ as a function of pressure is a measure of the pressure dependence of $\underline{K}$. Thus $\underline{k}$ is a highly interesting thermodynamic parameter. In Fig.15a $\underline{k}$ is plotted on a logarithmic scale versus pressure $\underline{p}$ for phenyl stearate on Perisorb RP8 as stationary phase (77-79). A rise in pressure from 9 to 19 MPa results in a decrease of the capacity ratio by about two orders of magnitude as a result of the rapidly increasing solvent power of supercritical carbon dioxide with increasing density. The logarithmic plot of $\underline{k}$ versus CO_2 density in Fig.15b gives nearly straight lines; the temperature dependence is small giving lower $\underline{k}$ values (that is higher $\underline{c}^{mob}$ values) with increasing temperature whereas for the plot against pressure in Fig.15a the temperature dependence is opposite. Additional results obtained for phenyl myristate and phenyl palmitate and for the stationary phase Perisorb A will be published and discussed in detail elsewhere (77,79). Since the capacity ratio $\underline{k}$ is the smaller the higher the molecular mass of the ester, separations are also possible. For details see references 76 to 79 and 84.

The use of a chromatographic technique for the determination of diffusion coefficients has been established in the early sixties and has been of considerable interest since then. Compared to static methods it offers a rapid approach to diffusion data and can be applied to gases, liquids, and supercritical phases as well as over a wide range of pressures and temperatures. The principle is to replace the usual separation column by an empty capillary tube of suitable length and diameter. In the absence of any stationary phase the dispersion of a sharp pulse of solute introduced into a laminary flow of the mobile phase is governed only by convective and diffusive mass transfer. In this case the mathematical treatment yields the simplified equation for the plate height $\underline{H}$

$$\underline{H} = \frac{2\underline{D}_{12}}{\bar{\underline{u}}} + \frac{\underline{r}_o^2\,\bar{\underline{u}}}{24\,\underline{D}_{12}} \qquad (11)$$

with

$$\underline{H} = \frac{\underline{\sigma}^2(\underline{x})}{\underline{l}} \qquad (12)$$

where $\underline{\sigma}^2(\underline{x})$ is the peak variance expressed as a length, $\bar{\underline{u}}$ the average velocity

of the mobile phase, r_o the inner radius and l the length of the capillary tube. In Fig.16 the binary diffusion coefficients D_{12} of some compounds in supercritical CO_2 at 313 K are plotted against density, the experimental range corresponding to pressures from 8 to 16 MPa. D_{12} values between 10^{-3} and 10^{-4} $cm^2.s^{-1}$ are found that decrease slightly with density. For comparison the self-diffusion coefficient D_{11} of carbon dioxide is also given in Fig.16 according to measurements of Robb et al. (85); it is larger than the D_{12} values shown by a factor of less than 10 only. For details and references see references 76 and 80 to 83.

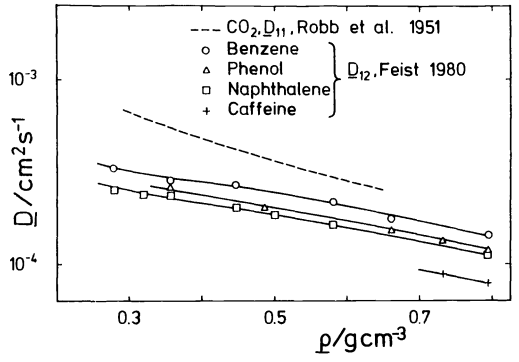

Fig. 16. Binary diffusion coefficient D_{12} of benzene, phenol, naphthalene, and caffeine in supercritical carbon dioxide as a function of density at 313 K (78,82). For comparison the self-diffusion coefficient D_{11} of carbon dioxide is also given (85).

CONCLUSION

Since there will certainly be further applications in the future, it seems worthwhile to stimulate interest in the physicochemical properties of fluid mixtures at high pressures. These properties, largely unknown up to now, really merit extensive investigation. Owing to rapid developments in experimental high-pressure techniques, the ranges of temperature and pressures involved are already accessible quite easily and at moderate costs. Informations about very recent work in this field can easily be obtained from the Bibliography on High Pressure Research (86). Please help to make pressure a "non-hidden" variable!

Acknowledgement -- Financial support of the Deutsche Forschungsgmeinschaft (DFG) and of the Fonds der Chemischen Industrie e.V. is gratefully acknowledged.

REFERENCES

1. F. Kohler, H. Kratzke, R. Niepmann and E. Spillner, paper presented at the IUPAC Conference on Chemical Thermodynamics, University College London, 6 to 10 September 82, Section 6, Paper 1. (The thermodynamic properties of liquid benzene).
2. D. Ambrose and N.C. Patel, as (1), Section 6, Paper 2. (Extrapolation of vapour pressures and estimation of critical pressures by the principle of corresponding states using two non-spherical reference fluids).
3. H. Kratzke, E. Spillner and S. Müller, as (1), Section 6, Paper 3. (The vapour pressure of liquid n-butane).
4. R. Vilcu and S. Perisanu, as (1), Section 6, Paper 4. (Thermodynamic study of the enthalpies of vaporization of carboxylic acids).
5. J.H. Dymond, N. Glen and J.D. Isdale, as (1), Section 6, Paper 5. ((p,ρ,T) and phase behaviour of some binary non-electrolyte mixtures).
6. J.J. Christensen and R.M. Izatt, as (1), Section 6, Paper 6. (Heats of mixing of binary systems near the critical point of one of the components).

7. G. Oswald and R.N. Lichtenthaler, as (1), Section 6, Paper 7. (The pressure dependence of the excess enthalpy of (alcohol + alkane)).
8. M.B. Ewing, R.N. Hurle and M.L. McGlashan, as (1), Section 6, Paper 8. (An apparatus for the rapid determination of fluid-fluid equilibrium).
9. H. Bijl, Th.W. de Loos and R.N. Lichtenthaler, as (1), Section 6, Paper 9. (Liquid + liquid equilibria in (2-methoxyethanol + an alkane) at high pressure).
10. A. Heintz and W.B. Streett, as (1), Section 6, Paper 10. (Phase equilibria in the systems (hydrogen + ethylene) and (hydrogen + ethane) at pressures up to 600 MPa).
11. M. Wirths, K.D. Wisotzki and G.M. Schneider, as (1), Section 6, Paper 11. (Fluid phase equilibria in binary (hydrocarbon + fluorocarbon) and (hydrocarbon + nitrogen) mixtures from 90 to 550 K and up to 250 MPa).
12. U. Deiters, as (1), Section 6, Paper 12. (Calculation of fluid phase equilibria in mixtures of small molecules at high pressures).
13. R. Koningsveld, L.A. Kleintjens, A.G. Swenker and M.G.G. Vanmeulenbrouk, as (1), Section 6, Paper 13. (Accurate mean-field treatment of the density of helium-4 close to and far from the critical point).
14. P. Keller, L.A. Kleintjens and R. Koningsfeld, as (1), Section 6, Paper 14. (Fluid-phase separations in two-component noble-gas mixtures; application of the mean-field lattice-gas model).
15. G.M. Schneider, Ber.Bunsenges. Phys. Chem., 70, 497-520 (1966).
16. G.M. Schneider, Fortschr. Chem. Forsch. 13, 559-600 (1970).
17. G.M. Schneider, Adv. Chem. Phys. 17, 1-42 (1970).
18. G.M. Schneider in Water - A Comprehensive Treatise, F. Franks ed., Vol. 2, Plenum Press, New York, 1973, Chap. 6, p. 381-404.
19. G.M. Schneider, Pure & Appl. Chem. 47, 277-291 (1976).
20. G.M. Schneider, Angew. Chem. Int. Ed. Engl. 17, 716-727 (1978).
21. G.M. Schneider, in Chemical Thermodynamics, Vol. 2, M.L. McGlashan ed., A Specialist Periodical Report, London, 1978, Chap. 4, p. 105-146.
22. G.M. Schneider in High Pressure Science and Technology, Vol. 1, K.D. Timmerhaus and M.S. Barber eds, Plenum, New York, 1979, p. 506-517.
23. G.M. Schneider, Vorträge N 301, Rheinisch-Westfälische Akademie der Wissenschaften, Westdeutscher Verlag, 1981, p. 7-49.
24. P. Engels and G.M. Schneider, Ber. Bunsenges. Phys. Chem. 76, 1239-1242 (1972).
25. G. Götze, Doctoral Thesis, University of Bochum, 1976.
26. G. Götze and P. Jeschke, Ber. Bunsenges. Phys. Chem. 81, 933-936 (1977).
27. P. Jeschke and G.M. Schneider, J. Chem. Thermodynamics 10, 803-808 (1978).
28. W. Ohling and G.M. Schneider, J. Chem. Thermodynamics 11, 305-306 (1979).
29. G. Götze and G.M. Schneider, J. Chem. Thermodynamics 12, 661-672 (1980).
30. G. Katzenski and G.M. Schneider, J. Chem. Thermodynamics 14, 801-802 (1982).
31. G. Katzenski and G.M. Schneider, J. Chem. Thermodynamics 14, 803-804 (1982).
32. D. Hess, Diploma Thesis, University of Bochum, 1982.
33. A. Heintz, Ber. Bunsenges. Phys. Chem. 85, 632-635 (1981).
34. P. Jeschke and G.M. Schneider, J. Chem. Thermodynamics 14, 157-165 (1982).
35. P. Jeschke and G.M. Schneider, J. Chem. Thermodynamics 14, 743-754 (1982).
36. C. Josefiak and G.M. Schneider, J. Phys. Chem. 83, 2126-2128 (1979); 84, 3004-3007 (1980).
37. J. Wenzel, Doctoral Thesis, University of Bochum, 1980.
38. J. Wenzel, U. Limbach, G. Bresonik and G.M. Schneider, J. Phys. Chem. 84, 1991-1995 (1980).
39. J. Wenzel and G.M. Schneider, Rev. Sci. Instrum. 52, 1889-1890 (1981).
40. Z. Alwani and G.M. Schneider, Ber. Bunsenges. Phys. Chem. 80, 1310-1315 (1976).
41. R. Jockers and G.M. Schneider, Ber. Bunsenges. Phys. Chem. 82, 576-582 (1978).
42. K.G. Liphard and G.M. Schneider, J. Chem. Thermodynamics 7, 805-814 (1975).
43. R. Paas, Z. Alwani, E. Horvath and G.M. Schneider, J. Chem. Thermodynamics 11, 693-702 (1979).
44. R. Paas and G.M. Schneider, J. Chem. Thermodynamics 11, 267-276 (1979).
45. K.H. Peter, R. Paas and G.M. Schneider, J. Chem. Thermodynamics 8, 731-740 (1976).
46. P. Jeschke, Doctoral Thesis, University of Bochum, 1980.
47. P. Jeschke and G.M. Schneider, J. Chem. Thermodynamics 14, 547-554 (1982).
48. A. Mukherjee, Ph. D. Thesis, Imperial College, London, 1978.
49. J.M.M. Mendonça, Ph. D. Thesis, Imperial College, London, 1979.
50. M. Wirths, Doctoral Thesis, University of Bochum, in preparation.
51. R. Stryjek, P.S. Chappelear and R. Kobayashi, J. Chem. Eng. Data 19, 334-339 (1974).
52. R. Stryjek, P.S. Chappelear and R. Kobayashi, J. Chem. Eng. Data 19, 340-343 (1974).
53. J.G. Roof and J.D. Baron, J. Chem. Eng. Data 12, 292-293 (1967).

54. W.W. Akers, L.L. Attwell and J.A. Robinson, I & EC 46, 2539-2540 (1954).
55. K.D. Wisotzki, Doctoral Thesis, University of Bochum, in preparation.
56. R.S. Poston and J.J. McKetta, J. Chem. Eng. Data 11, 364-365 (1966).
57. S. Peter and H.F. Eicke, Ber. Bunsenges. Phys. Chem. 74, 190-194 (1970).
58. I. Swaid, Doctoral Thesis, University of Bochum, in preparation.
59. R. Konrad, I. Swaid and G.M. Schneider, paper presented at the Meeting of the Industrial Physical Chemistry Group, Faraday Division, Royal Society of Chemistry on "Supercritical Fluids: Their Chemistry and Application". Girton College, Cambridge, 13-15 September 1982; Fluid Phase Equilibria, in press.
60. R. Konrad, Doctoral Thesis, University of Bochum, 1982.
61. C. Reid, J.M. Prausnitz and T.K. Sherwood, The Properties of Gases and Liquids, McGraw-Hill, New York, 1977.
62. C.F. Spencer, T.E. Daubert and R.P. Danner, A.I.Ch.E.J. 19, 522-527 (1973).
63. N.J. Trappeniers and J.A. Schouten, Physica 73, 546 (1974).
64. U. Deiters, Doctoral Thesis, University of Bochum, 1979.
65. U. Deiters, Chem. Eng. Sci. 36, 1139-1146, 1147-1151 (1981); 37, 855-861 (1982).
66. U. Deiters and G.M. Schneider, Ber. Bunsenges. Phys. Chem. 80, 1316-1321 (1976).
67. U. Deiters, Fluid Phase Equilibria 8, 123-129 (1982).
68. K.E. Gubbins and C.H. Twu, Chem. Eng. Sci. 33, 863-878 (1978); C.H. Twu and K.E. Gubbins, Chem. Eng. Sci. 33, 879-887 (1978).
69. G.M. Schneider in Experimental Thermodynamics, B. Le Neindre and B. Vodar eds., Butterworth, London, 1975, Chap. 16, Part 2.
70. C.L. Young in Chemical Thermodynamics, Vol. 2, M.L. McGlashan ed., A Specialist Periodical Report, The Chemical Society, London, 1978; Chap. 3.
71. Z. Alwani, Rev. Sci. Instrum. 49, 944-947 (1978).
72. Extraction with Supercritical Gases, G.M. Schneider, E. Stahl and G. Wilke eds., Verlag Chemie, Weinheim, 1980.
73. Angew. Chemie Int. Ed. Engl. 17 (10), 701-754 (1978).
74. Sep. Sci. Techn. 17 (1) (1982).
75. G. Brunner and S. Peter, Chem. Ing.-Techn. 53, 529-542 (1981).
76. U. van Wasen, I. Swaid and G.M. Schneider, Angew. Chem. Int. Ed. Engl. 19, 575-587 (1980).
77. A. Wilsch, Diploma Thesis, University of Bochum, 1982.
78. A. Wilsch, R. Feist and G.M. Schneider, paper presented at the Meeting of the Industrial Physical Chemistry Group, Faraday Division, Royal Society of Chemistry, on "Supercritical Fluids: Their Chemistry and Application", Girton College, Cambridge, 13-15 September 1982; Fluid Phase Equilibria, in press.
79. A. Wilsch and G.M. Schneider, Z. Anal. Chem., submitted for publication.
80. U. van Wasen and G.M. Schneider, J. Phys. Chem. 84, 229-230 (1980).
81. I. Swaid and G.M. Schneider, Ber. Bunsenges. Phys. Chem. 83, 969-974 (1979).
82. R. Feist and G.M. Schneider, Sep. Sci. Techn. 17, 261-270 (1982).
83. R. Feist, Doctoral Thesis, University of Bochum, in preparation.
84. D.R. Gere, Anal. Chem. 54, 736-740 (1982).
85. W.L. Robb and H.G. Drickamer, J. Chem. Phys. 19, 1504-1508 (1951).
86. Bibliography on High Pressure Research, High Pressure Data Center, Leo Merril, Director, P.O.Box 7246, University Station, Provo, Utah 84602-0246, USA.
87. U. Deiters, University of Bochum, private communication.